Materials Today Communications 25 (2020) 101469

Contents lists available at ScienceDirect

Materials Today Communications

journal homepage: www.elsevier.com/locate/mtcomm

Effect of kaolin geopolymer ceramic addition on the properties of Sn-3.0Ag-0.5Cu solder joint

N.S. Mohamad Zaimi[a], M.A.A. Mohd Salleh[a,*], M.M.A.B. Abdullah[a], R. Ahmad[b], M. Mostapha[a], S. Yoriya[c], J. Chaiprapa[d], G. Zhang[e], D.M. Harvey[e]

[a] Center of Excellence Geopolymer & Green Technology (CeGeoGTech), School of Materials Engineering, Universiti Malaysia Perlis (UniMAP), Taman Muhibbah, 02600 Jejawi, Arau, Perlis, Malaysia
[b] Faculty of Engineering Technology, Uniciti Alam Campus, Universiti Malaysia Perlis (UniMAP), Perlis, Malaysia
[c] National Metal and Materials Technology Center, National Science and Technology Development Agency, 114 MTEC, Thailand Science Park, Pahonyothin Road, Khlong Neung, Khlong Luang, Pathum Thani 12120, Thailand
[d] Synchrotron Light Research Institute, Muang District, Nakhon Ratchasima, 3000, Thailand
[e] General Engineering Research Institute, Liverpool John Moores University, Byrom Street, L3 3AF, United Kingdom

ARTICLE INFO

Keywords:
Geopolymer ceramics
Solder material
Soldering
Intermetallics
Microstructure

ABSTRACT

This paper investigates the effects of different weight percentages (0, 0.5, 1.0, 1.5 and 2.0 wt.%) of kaolin geopolymer ceramic (KGC) on the microstructure formation, thermal properties, spreadability and joint strength in Sn-3.0Ag-0.5Cu (SAC305) lead-free solder alloys in order to develop a new composite solder system. Advanced characterization techniques such as Electron backscatter diffraction (EBSD) and synchrotron micro-XRF were used to study the behaviors of the pure SAC305 and KGC reinforced SAC305 composite solders. Experimental results shows that the addition of KGC refines the β-Sn area and increases the eutectic area with fine intermetallics formation. In addition, the thickness of the IMC layer is reduced with a reduction in undercooling value for the KGC reinforced SAC305 composite solder. The spreadability of the KGC reinforced SAC305 composite solder is significantly increased in the spreadable area with a higher strength of solder joint. Significantly, the results obtained prove that 1.0 wt.% KGC addition gives better performance in terms of microstructure formation, thermal properties, spreadability and joint strength. Synchrotron micro-XRF interestingly indicated that some Al and Si, which are the major elements in geopolymer systems, migrate into the solder area.

1. Introduction

The transition to lead free solder alloy has been at the forefront of peoples minds for more than a decade due to the prohibition in the consumption of lead in solder alloy by Restriction of Hazardous Substance (RoHS) and The Waste of Electrical and Electronic Equipment (WEEE) in the electronic packaging industries [1]. This triggered extensive research to develop a 'green' solder alloy. Among the various emerging lead free solders, Sn-Ag-Cu (SAC) lead free solder alloy posed the outstanding choice by the industry to replace conventional Sn-Pb solder alloy because SAC solder alloy show good wettability, better solder joint strength and lower melting point than the other Sn-based solder alloys [1–5]. However, the performance of SAC could not meet or perform better than conventional lead solder especially during thermal cycling [6]. On top of that, other major concerns related with SAC are the formation of large and brittle intermetallic compounds (IMCs) of Cu_6Sn_5 rods and Ag_3Sn plates, promotes by higher undercooling of β-Sn (~10 − 40 K) in turns reduce the mechanical strength and solder reliability [4,7]. Since IMCs are brittle, controlling its growth is necessary in obtaining a strong and reliable solder joint.

Currently, microelectronic devices are becoming more complicated with miniaturization, which continually reduces the sizes of the solder interconnections. Significant research work has been done in finding suitable and compatible solder alloys to replace the conventional tin lead solder, and to fulfill the demands of highly reliable solder alloys for use in complex and future microelectronic devices. Recently, the emergence of composite solder technology has attracted much interest worldwide. The introduction of reinforcing particles, which are either metals or non-metals, into the matrix of a solder alloy by forming composite solder were considered likely candidates to improve the performance and properties of existing solder alloys. Generally,

* Corresponding author.
E-mail address: arifanuar@unimap.edu.my (M.A.A. Mohd Salleh).

https://doi.org/10.1016/j.mtcomm.2020.101469
Received 20 April 2020; Received in revised form 2 July 2020; Accepted 14 July 2020
Available online 17 July 2020

reinforcing the matrix of solder alloys with ceramic particles gained an interest among the researchers as a method to improve the existing solder alloy properties. This was due to the fact that ceramic reinforcements were extremely stable at high temperature and no new excessive phase were formed either during fabrication or due to the large temperature difference between the reinforcing particles and solder alloys [4,5]. Reinforcing the solder matrix with small amounts of ceramic particles including cerium oxide (CeO_2) [8,9], zirconia (ZrO_2) [10,11], titanium oxide (TiO_2) [5,12–14], silicon carbide (SiC) [15,16], silicon nitride (Si_3N_4) [17,18], iron oxide (Fe_2O_3) [19], strontium titanate ($SrTiO_3$) [20], titanium carbide (TiC) [21], silicon dioxide (SiO_2) [22], lanthanum oxide (La_2O_3) [23] and aluminium oxide (Al_2O_3) [24,25] have shown to improve microstructure formations, mechanical and thermal properties of solder. Li et al. [8] hypothesized that the incorporation of ceramic particles in solder matrix may act as heterogenous nucleation sites for β-Sn and eutectic phase which could increase the nucleation rate and may result in smaller grain size. Moreover, S.S. Mohd Nasir et al. [12] reported that, TiO_2 ceramic particles able to improve mechanical strength as the refined Ag_3Sn and Cu_6Sn_5 IMCs able to restrict dislocation motion. Besides that, Gain et al. [11] has hypothesized that the shear strength of Sn-Ag-Cu was higher than for unreinforced solder even though it was subjected to multiple reflow cycles, due to the homogenous distributions of ceramic particles that lead to a dispersion strengthening mechanism. It was also proved that ceramics particles could absorb the molten solder during the soldering process, thereby limiting substrate dissolution and diffusion which could decrease the thickness of interfacial IMC layer and be beneficial to the strength of solder joints [26].

Geopolymer is an inorganic polymer material that formed through a geopolymerization process involving the dissolution of aluminosilicate sources material which consist of SiO_2 and Al_2O_3 in highly alkaline activated solution producing amorphous to semi-crystalline structures with Si-−O-Al and Si-O-S−−−i bonds [27]. Interestingly, geopolymer powder can be used to produce geopolymer ceramics through a sintering process yielding crystalline phases, which require slightly lower sintering temperatures, but with excellent mechanical properties compared to typical ceramics [28–30]. This fabrication process was beneficial towards reducing the consumption of high energy for the production of ceramics [31]. In addition, geopolymer ceramic consists of elements which may act as additional nucleation sites to improve the properties of solder alloys. Various hypotheses have been suggested on the incorporation of ceramic particles to existing solder alloys. However, to the best of the authors' knowledge, there is no research reported on the effect of using kaolin geopolymer ceramic as the reinforcement particles, and on how that may positively affect existing solder alloys. Thus, this paper aims to investigate the effect of geopolymer ceramics as the potential reinforcement particles in Sn-Ag-Cu solder alloys which could improve the microstructure, thermal and mechanical properties of Sn-Ag-Cu solder alloys.

2. Experimental procedure

2.1. Sample preparation

In this research, Sn-3.0Ag-0.5Cu (SAC305) solder powders with an average particle size in the range between 25–45 μm were used as the base matrix material. Kaolin geopolymer ceramics with an average particle size of 18.41 μm were used as reinforcement materials. The kaolin geopolymer ceramics (KGC) powder were controlled by sieving the powder with a 38 μm siever. The particle size were then measured using ImageJ software on scanning electron microscope (SEM) images. The distributions of the particle size for SAC305 and KGC powder were presented in Fig. 1(c) and (d). Kaolin (supplied by Associated Kaolin Industries Sdn Bhd, Malaysia) were used as raw materials in the production of kaolin geopolymer ceramics. Then, kaolin was mixed with an alkaline activator solution and cured at temperature of 80 °C for 24 h to form kaolin geopolymer. The kaolin geopolymer were then crushed by a mechanical crusher, compacted by using uniaxial pressing with a load of 4.5 tons and sintered at a temperature of 1200 °C with 180 min of soaking time to form kaolin geopolymer ceramics. Then, the sintered KGC underwent ball milling in a planetary mill machine for 10 h with a speed of 450 rpm and ball to powder ratio of 10:1, so as to produce kaolin geopolymer ceramic powders with a size of less than 38 μm. The morphology of SAC305 and KGC are shown in Fig. 1(a) and (b), respectively. The chemical composition of raw KGC powder based on laboratory X-ray fluorescence (XRF) was listed in Table 1. The main chemical compositions of KGC were Al_2O_3 and SiO_2, smaller amounts of Na_2O, K_2O and Fe_2O_3.

The fabrication of SAC305/kaolin geopolymer ceramics composite solder were done by using a powder metallurgy route. Various weight percentage (wt.%) of kaolin geopolymer ceramics (0, 0.5, 1.0, 1.5 and 2.0 wt.%) were homogeneously mixed in an air tight container by using a planetary mill at a speed of 200 rpm for an hour. The solder mixtures were uniaxially compacted in a 12 mm stainless steel mold by using a Specac-15-Ton Manual Hydraulic Press with a load of 4.5 tons. Then, the compacted pellets were sintered by using a hybrid microwave sintering technique at 185 °C under ambient conditions by using 800 W, 50 Hz Panasonic oven for 3 min. A microwave susceptor material of silicon carbide (SiC) was used in this study.

2.2. Microstructure analysis

The microstructure of compacted sintered pellets was analyzed by using a scanning electron microscope (SEM) in backscattered electron imaging mode in order to observe the distributions of kaolin geopolymer ceramics. The pellets were etched by using a dilute solution of 2% hydrochloric acid (HCl), 5% nitric acid (HNO_3) and 93 % methanol (CH_3OH) in order to have a clear grain boundary observation. In fabricating solder balls, compacted sintered pellets were rolled into thin sheets with a thickness of approximately 50 μm. The thinned sheets were punched by using a 3.0 mm puncher in order to prepare a 900 μm diameter solder ball. The punch sheets were then dipped in rosin mildly activated flux (RMA) and melted on Pyrex plate at a temperature of 250 °C in a reflow oven. Solder balls with a spherical shape were formed due to the action of surface tension during melting of the solder samples. Subsequently, the solder balls were sieved using siever of 1 mm and 0.9 mm size in order to obtain a uniform size of solder balls. In order to form solder joints, the fabricated solder balls were reflowed on a 900 μm ball pitch size of Cu substrate printed circuit board (PCB) with an organic solderability perspective (OSP) surface finish and a small amount of RMA flux applied prior to the reflow soldering process. The reflow soldering process was carried out on 5 samples for each of compositions by using a F4N desktop reflow oven at a temperature of 250 °C (time above liquid is 25 s). The reflowed samples were cross-sectioned, cold-mounted in epoxy resin, ground with SiC paper and polished. The microstructures of reflowed samples were analysed with scanning electron microscope (SEM), electron backscattered diffraction (EBSD) and Synchrotron Micro-XRF (μ-XRF).The morphology and thickness of interfacial intermetallic compounds (IMC) layer of the solder joints were observed using a scanning electron microscope (SEM). The thickness of IMC layer was evaluated by using J-Image software. The measurements of IMC thickness (t) were calculated as the area of IMC (A) divided with the length of IMC (L). Five samples for each of compositions were used to measure the average thickness of IMC layer.

Electron backscattered diffraction (EBSD) samples were firstly ion-milled by Hitachi IM-4000 ion milling equipment for about 10 min with a rotation speed of 25 rpm. Then, the regions of solder ball were covered by a conductive layer of carbon in order to eliminate the effects of charging. During the EBSD testing, the samples were tilted to 70° and an Hitachi SU8230 scanning electron microscope equipped with Nordlys EBSD detector, operated at 25 kV used. For EBSD acquisition, a step size

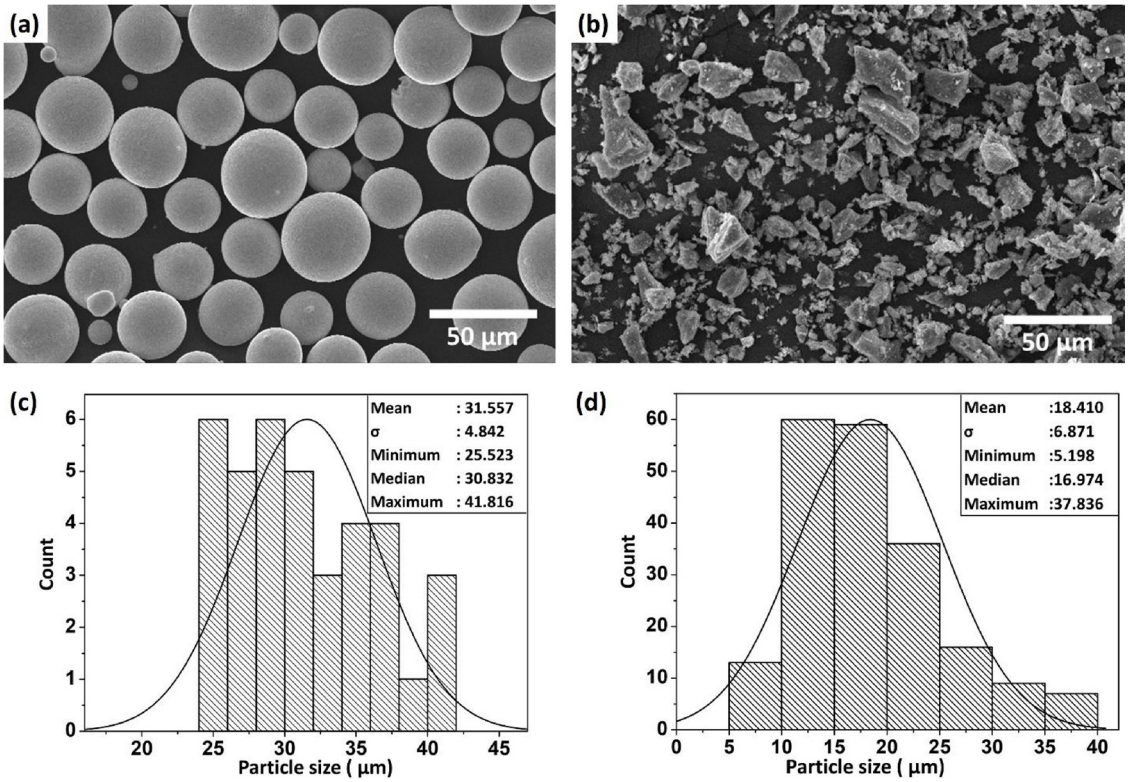

Fig. 1. Morphology of (a) SAC305 solder powder, (b) kaolin geopolymer ceramic powder, (c) particle size distributions of SAC305 solder powder and (d) particle size distributions of kaolin geopolymer ceramic powder.

Table 1
Chemical composition of kaolin geopolymer ceramic powder by using X-ray fluorescence.

Compound	Content (wt.%)
Na_2O	4.5
Al_2O_3	31.9
SiO_2	56.6
K_2O	2.50
TiO_2	0.74
MnO_2	0.05
Fe_2O_3	2.83
ZrO_2	0.05
LOI	0.83

of 1.5 µm was chosen, with Emax Evolution software used for the analysis.

In order to investigate the interactions of kaolin geopolymer ceramic (KGC) to Sn-3.0Ag-0.5Cu (SAC305) lead free solder, a small bar of bulk KGC (5 × 10 × 30 mm) was dipped in molten SAC solder at 250 °C for approximately 10 min and subsequently cooled in air. Then, the samples were carefully fine polishing before it was analysed under synchrotron micro-XRF (µ-XRF). The schematic diagram for the experimental setup is shown in Fig. 2. To precisely analyse the interaction between KGC to SAC solder, a detail elemental distribution analysis using synchrotron micro-XRF. By using synchrotron radiation and 30 × 30 μm^2 size of beam focused by the polycapillary lens, the element distributions in the solder was obtained. Samples were placed at a 90° level between the X-ray and the CCD camera. A Vortex EM-650 silicon drift detector was used to collect the emitted fluorescence X-Ray and the area of interest was accurately specified by using high precision motorized stages. A 0.05 mm scanning step with an exposure time of 10 s for each point was used. PyMca software was used to analyse the data obtained. The area of interest of the sample, with a size of 750 µm X 700 µm was scanned during synchrotron micro-XRF testing.

Solderability of all the samples were investigated by measuring a spreading area on copper (Cu) substrate. A Cu substrate of 30 mm x 30

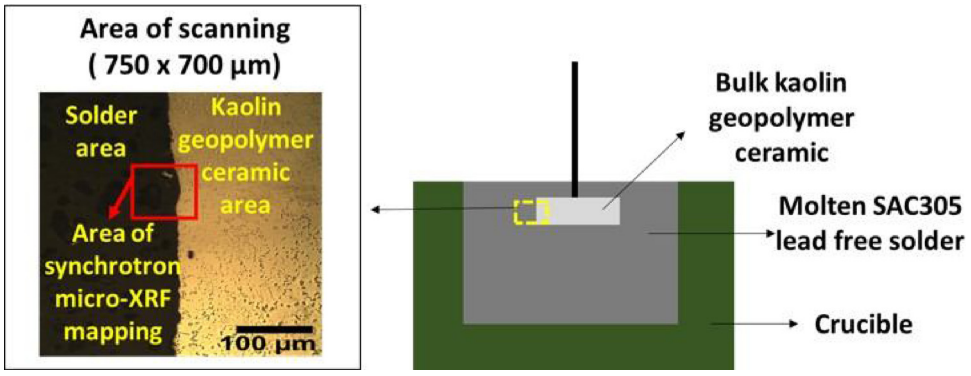

Fig. 2. Schematic diagram for the experimental setup dipping of bulk kaolin geopolymer ceramic in SAC305 lead free solder.

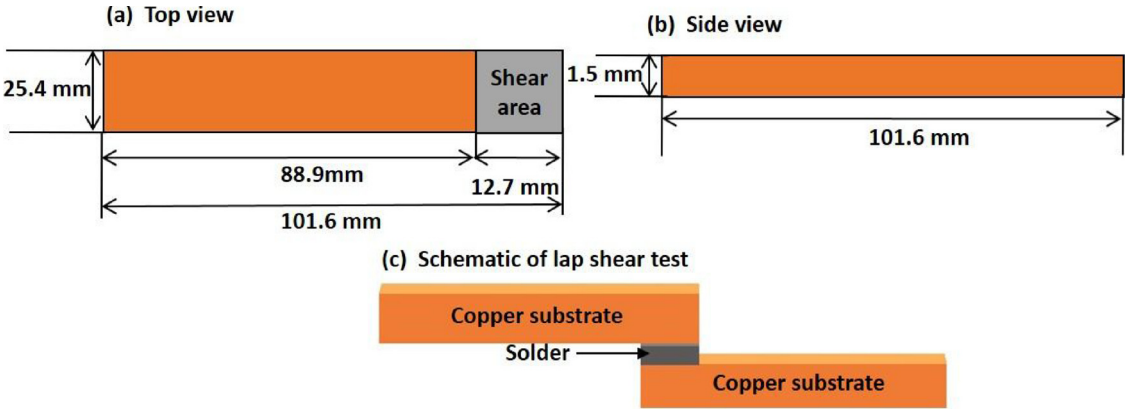

Fig. 3. (a) and (b) Specifications of Cu-substrate (FR4-Type PCB) used for shear test and (c) schematic diagram of single-lap shear test.

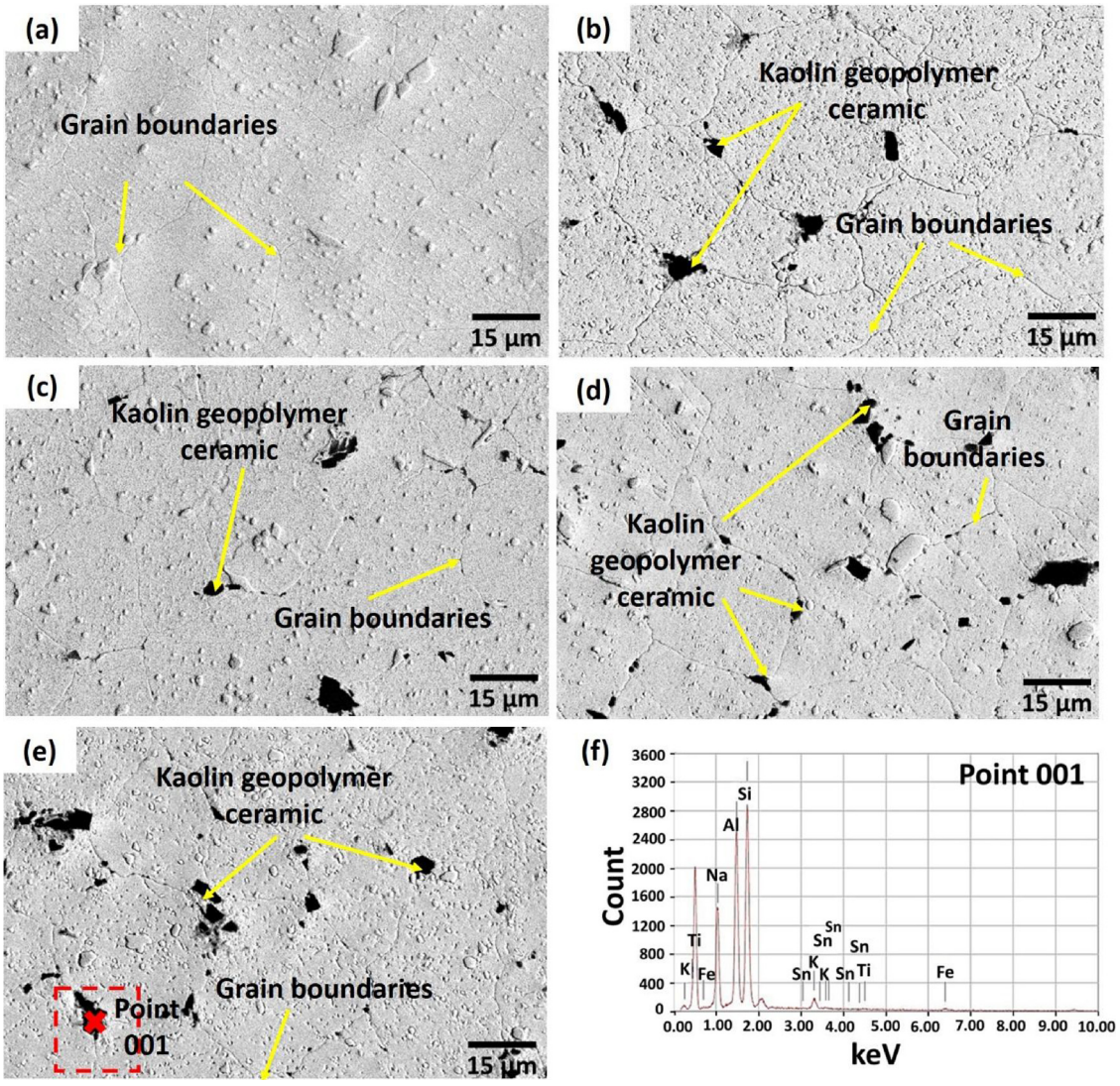

Fig. 4. SEM micrograph of sintered SAC305/kaolin geopolymer ceramic samples showing distribution of KGC at (a) 0 wt.% KGC, (b) 0.5 wt.% KGC, (c) 1.0 wt.% KGC, (d) 1.5 wt.% KGC, (e) 2.0 wt.% KGC and (f) EDX point analysis at Point 001.

mm x 0.3 mm was used in this study. The Cu substrate was finely polished and cleaned with the acid cleaning liquid which consists mixture of 5 g hydrochloric acid and 95 g deionized water to remove surface impurities on Cu substrates. Subsequently, 0.3 g of solder sheets were placed on Cu substrates with 0.03 g RMA flux. The samples were then reflowed in a F4N reflow oven and the spreading areas were measured using J-Image software. A total of five samples were tested for each of compositions.

2.3. Thermal properties analysis

The melting characteristics of all the samples were characterized by

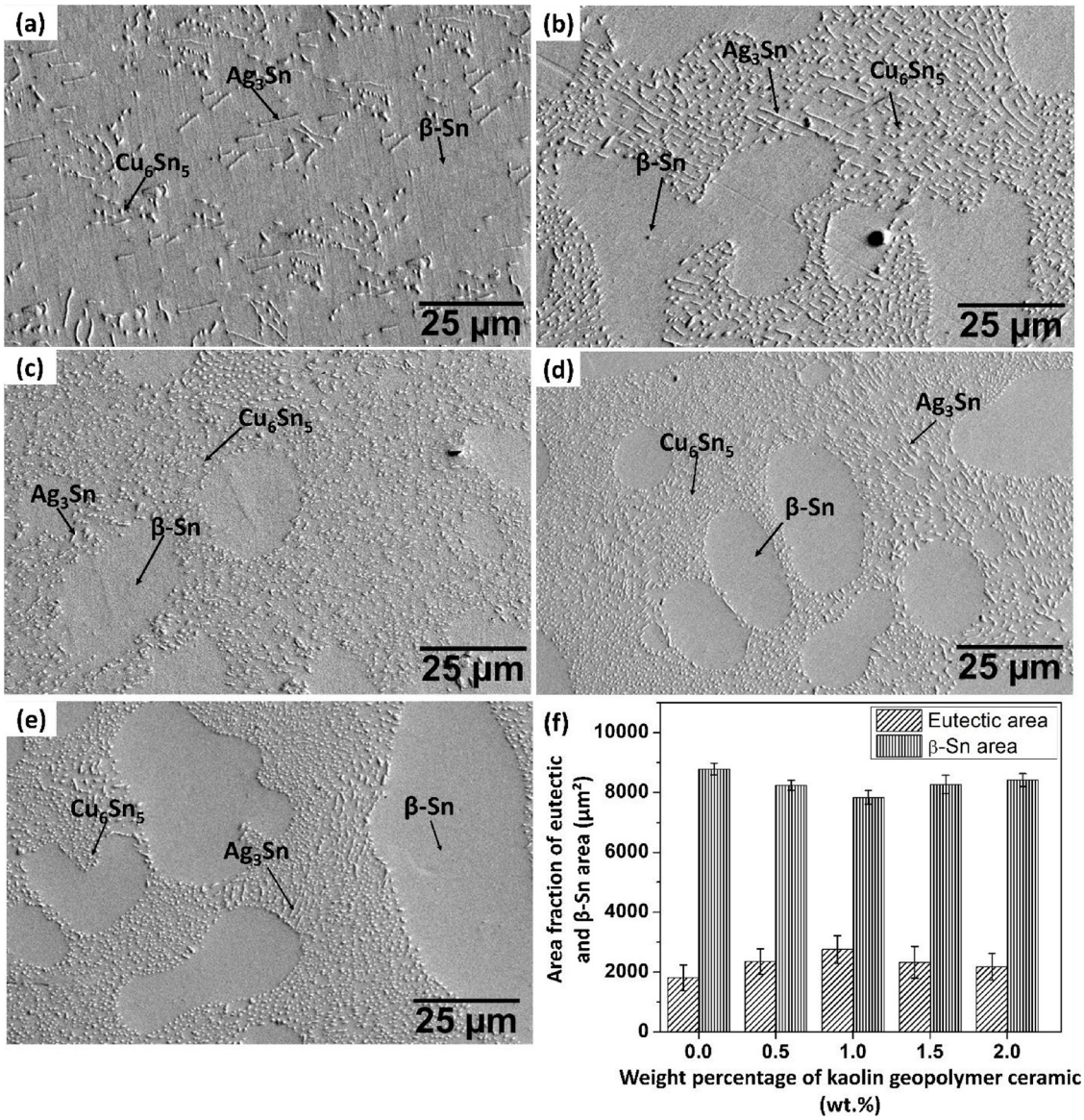

Fig. 5. Microstructure of SAC305 with additions of (a) 0 wt.%, (b) 0.5 wt.%, (c) 1.0 wt.%, (d) 1.5 wt.%, (e) 2.0 wt.% of KGC after reflowed on Cu substrate and (f) area fraction of eutectic and β-Sn area.

using a TA Instruments Differential Scanning Calorimetry (DSC). The weight for each of the samples were kept below 5 mg according to the requirement of DSC equipment and placed into an aluminum pan. All the samples were heated up to 250 °C and immediately cooled down to room temperature with a heating rate of 10 °C/min under a nitrogen gas (N_2) atmosphere.

2.4. Mechanical properties test

A single-lap shear solder joint test was performed to evaluate the strength of the solder joints which were bonded to the Cu substrate (PCB FR4-type). The single-lap shear test was conducted by using an Instron machine with the specifications of Cu substrate used as according to ASTM D1002 standard. According to the ASTM standard, the measurements of Cu substrate of 101.6 mm x 25.4 mm x 1.5 mm (Fig. 3) was used. Reflow soldering process was performed and the fracture analysis after the shear test was analyzed by using a scanning electron microscope.

3. Results and discussions

3.1. Microstructure and phase analysis

Microstructure formations in the developed Sn-3.0Ag-0.5Cu (SAC305) composite solders were analyzed based on post sintered and post reflowed samples. The sintered samples were etched and observed using a Scanning electron microscope (SEM). Fig. 4 depicts the micrograph of SEM for the post sintered pure SAC305 and KGC reinforced SAC305 composite solders with different weight percentage (wt.%) of kaolin geopolymer ceramic (KGC). It was observed the KGC particles, indicated as black particles, are well distributed along the grain boundaries in the samples with the addition of KGC in Fig. 4(b–e). The presence of these distributed black particles indicated as KGC was proved by EDX analysis in Fig. 4(f). The existence of Na, Al, Si, K, and Fe by EDX corresponds to the elements in KGC systems. In addition, the reinforcement concentrations along the grain boundaries tend to hold the grains, hence preventing grain dislocations which retards the growth of grains in the SAC305 solder matrix. Thus, the addition of KGC to a SAC305 solder matrix can improve the mechanical properties

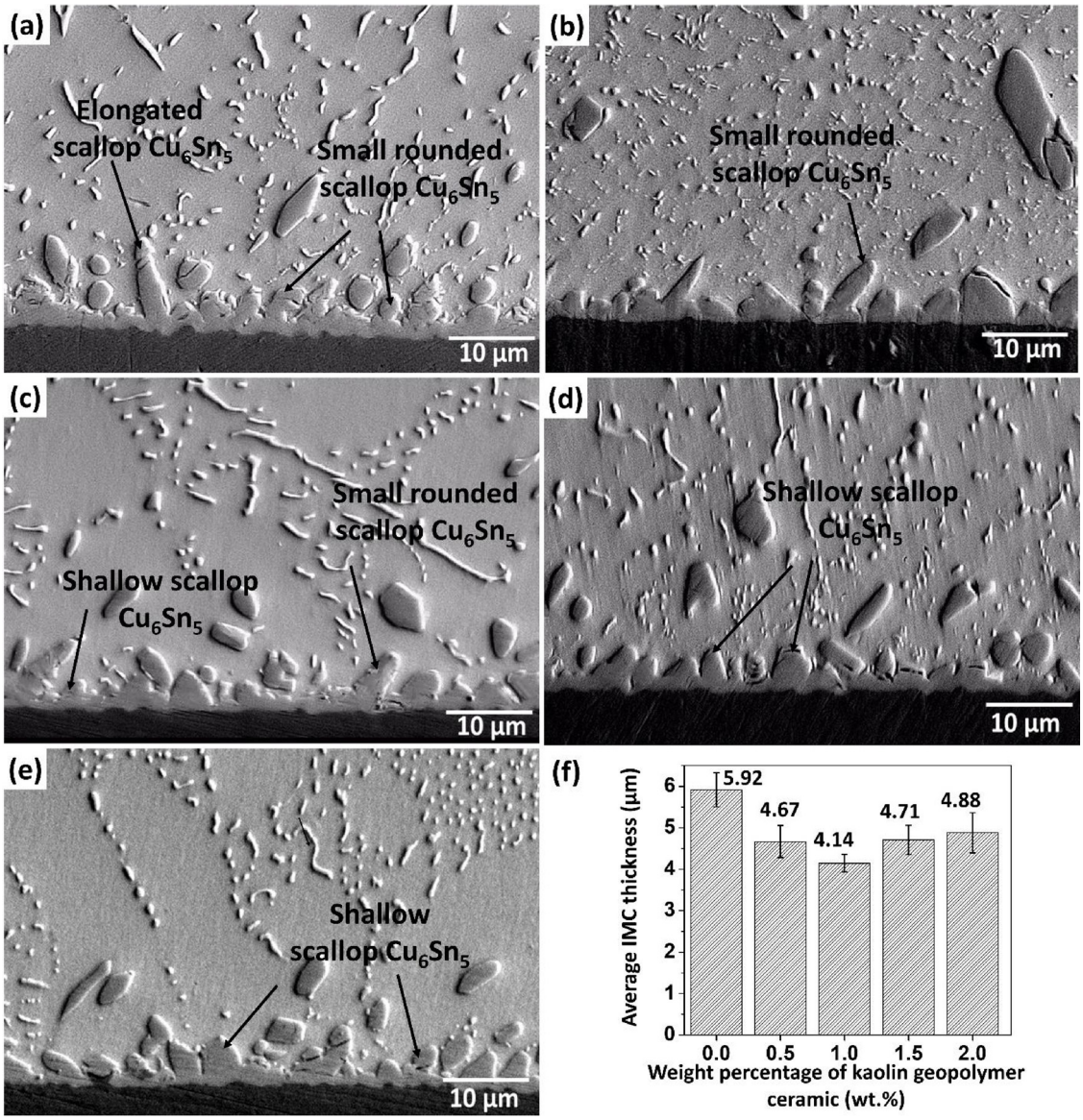

Fig. 6. Interfacial Cu_6Sn_5 IMC layer at different weight percentage of KGC; (a) 0 wt.%, (b) 0.5 wt.%, (c) 1.0 wt.%, (d) 1.5 wt.%, (e) 2.0 wt.% KGC and (f) average of IMC thickness with different wt.% KGC.

of solder.

To analyze the effect of adding KGC to the microstructures of SAC305 solder after reflow soldering, cross-sectional images of pure SAC305 and KGC reinforced SAC305 composite solder were observed by a scanning electron microscope, synchrotron micro-XRF and electron backscattered diffraction. Fig. 5 shows the backscattered SEM image of post-reflowed samples. Based on Fig. 5, it confirmed there existed two different phases in each of the cross-sectioned samples. The two phases were primary β-Sn phase and eutectic phase. In the eutectic phase, primary intermetallic compound (IMC) of Cu_6Sn_5 and Ag_3Sn are dispersed in the eutectic area. The addition of KGC particles to the SAC305 lead-free solder greatly refined the β-Sn phase and also reduced the size of primary Cu_6Sn_5 and Ag_3Sn. This indicated that the addition of KGC particles into SAC305 lead-free solder contributes to the refinement effect in the microstructures of solder. Moreover, to precisely observe the microstructural changes in each of the samples, the area fraction of β-Sn phases and eutectic phases were quantitatively analyzed with the help of thresholded images by using the J-image software. The area fraction of each phases were presented as depicted in Fig. 5(f). According to Fig. 5(f), additions of KGC particles influenced the area fraction of β-Sn and eutectic phases, in which the area fraction of β-Sn phases was slightly decreased with increased in the area fraction of eutectic phases (with smaller size of Cu_6Sn_5 and Ag_3Sn that dispersed in eutectic area) as the addition of KGC was up to 1.0 wt.%. However, as the amount of KGC added beyond 1.0 wt.% (in case of 1.5 wt.% and 2.0 wt.%), the area fraction of β-Sn phase increased with the decreased in the area fraction of eutectic phase. So, the addition of 1.0 wt.% KGC resulted in the best refinement of microstructures in the SAC305 lead free solder.

The enhancement in the microstructure of SAC305 lead free solder is likely attributed to the heterogeneous nucleation [8,17,32,33]. During the reflow soldering, KGC particles were segregated in the molten solder matrix. According to the theory of heterogenous nucleation, the presence of KGC particles in an alloy of SAC305 solder matrix act as heterogeneous nucleation sites for β-Sn and eutectic phases. The β-Sn and eutectic phases may nucleate on the surface of KGC particles as a means to reduce the thermodynamic barrier of nucleation as suggested by Li et.al [34]. Hence, the nucleation rate was increased, reducing the size of the grains. Moreover, the higher nucleation rate of grains prevents the grains ripening, which consequently

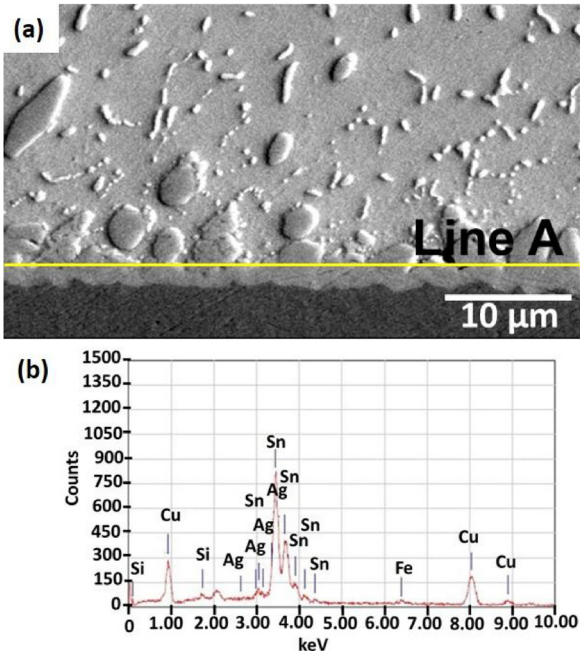

Fig. 7. (a) Cross-sectional view of EDX line at interfacial IMC layer and (b) EDX spectrum along the interfacial IMC layer at Line A.

results with refined microstructures in SAC305 solder with addition of KGC particles. A similar phenomenon was also reported by Wang et al. [22], where addition of SiO_2 effectively served as the grain refinement in solder alloys which may advantageously improve shear properties of composite solder alloys. The best microstructure refinement was achieved with 1.0 wt.% KGC, since the addition of KGC beyond this value slightly increases the area fraction β-Sn and decreases the area fraction of eutectic phase. An increase in particles can cause agglomeration of fine reinforcement particles in the Sn solder matrix which may decrease the surface energy and consequently reduce the refining effect in the solder [8].

An intermetallic compound (IMC) layer forms from the reaction between molten solder and copper (Cu) substrate during the soldering process [35]. The formation of an IMC layer is vital in a solder joint since it indicates the existence of metallurgical bonding between the solder and substrate. Nevertheless, an excessive formation of IMC layer is adverse to solder joint reliability. In this research, the IMC layer formed in the pure SAC305 solder and KGC reinforced SAC305 composite solder joints were analyzed based on the morphology and thickness of IMC layer. It can be observed from Fig. 6(a), the morphology of interfacial Cu_6Sn_5 layer consists of elongated and small scallop Cu_6Sn_5. However, as various weight percentage of KGC were added, the morphology of interfacial layer shows changes to the combination of shallow and small scallops as in Fig. 6(b–e). No formation of elongated scallop is observed in the KGC reinforced SAC305 composite solder. The formation of the elongated scallop was undesirable since the elongated scallop will induce brittle fractures to the solder joint and contribute to crack initiation sites. As a result it adversely affects the performance of solder joints [8,9]. The growth of elongated scallop at the interfacial layer can be caused by an increase in the concentration of copper atoms from a substrate which diffuses to the solder matrix and reacts with tin, resulting in growth of elongated scallop Cu_6Sn_5 [9].

The average thicknesses of IMC layer for pure SAC305 solder and KGC reinforced SAC305 composite solder as measured are shown in Fig. 6(f). Results proved that the thickness of IMC layer substantially decreased with the addition of KGC. The lowest average thickness of IMC layer was achieved with the addition of 1.0 wt.% KGC to the SAC305 solder. The reduction of 30 % on average of IMC layer thickness was observed with the addition of 1.0 wt.% KGC in comparison to the pure SAC305 solder. However, the average thickness of IMC layer in the KGC reinforced SAC305 composite solder slightly increased as the KGC added was beyond 1.0 wt.%. It is worthwhile to note that the reduction of the IMC layer thickness in the KGC reinforced SAC305 composite solder was ascribed to the effect of the added KGC. The existence of KGC particles was proven by using the EDX line analysis along the interfacial layer as shown in Fig. 7. The presence of Si and Fe elements by EDX analysis was due to the KGC particles. Therefore, it indicates that the presence of KGC along the interfacial IMC layer may suppress the growth of interfacial IMC during the soldering process.

The interfacial Cu_6Sn_5 IMC grains nucleate when the molten solder contacts with Cu substrate during the reflow soldering process, that results in a continuous IMC layer coverage at the Cu substrate/solder interface. As the concentration of Cu in SAC305 solder is less than 0.9 wt.%, the growth of scallop Cu_6Sn_5 IMC grains at the interface between substrate/solder required Cu atoms from the substrate to be dissolved simultaneously to the solder matrix [9]. In this case, the channels between the scallop Cu_6Sn_5 grains facilitated the growth of interfacial IMC in which it acts as the diffusion and dissolution paths for Cu atoms from the substrate to the solder matrix, as suggested by Hsiao et.al (2011) [36]. Thus, the existence of KGC particles along the interfacial IMC layer as shown in Fig. 7 may acts as a barrier which reduces the diffusion of Cu from the substrate to the solder matrix and thus limits the growth of interfacial IMC. As a result, a thinner thickness of interfacial IMC is obtained in the KGC reinforced SAC305 composite solder than the pure SAC305 solder. Besides that, the suppression of the interfacial IMC was partly owing to the KGC reinforced SAC305 composite solder solidifying at a lower undercooling than pure SAC305 solder as demonstrated by DSC results in Table 2.

In order to determine the elemental distribution of Sn, Ag, Cu and other elements in KGC systems for as-reflowed samples, a higher precision elemental mapping analysis was carried out using a synchrotron radiation source. Fig. 8 shows the results obtained using a synchrotron micro-XRF from pure SAC305 solder and KGC reinforced SAC305 composite solder. A higher intensity shown as counts, indicates higher distributions for a specific element. From Fig. 8(b) the elements of Al, Si, K, and Fe are clearly observed, which come from the KGC systems, as proved by the laboratory X-ray fluorescence (XRF) in Table 1. These elements were dominantly distributed in the region of the solder bulk area and only a little along the interfacial IMC of the solder joint. The existence of these elements in the KGC reinforced SAC305 composite solder further proved that, KGC particles can alter the microstructure formation, enhancing the properties of KGC reinforced SAC305 composite solder.

Table 2
Average undercooling,pasty range and melting temperature from DSC testing of SAC305 and KGC reinforced SAC305 composite solder with different weight percentages of kaolin geopolymer ceramic.

Solder	Average undercooling (°C)	Average pasty range (°C)	Average melting temperature (°C)
SAC305	19.64	8.92	220.86
SAC305 + 0.5 wt.% KGC	15.38	8.52	220.55
SAC305 + 1.0 wt.% KGC	14.89	8.50	220.56
SAC305 + 1.5 wt.% KGC	16.76	8.48	221.01
SAC305 + 2.0 wt.% KGC	16.81	8.91	221.11

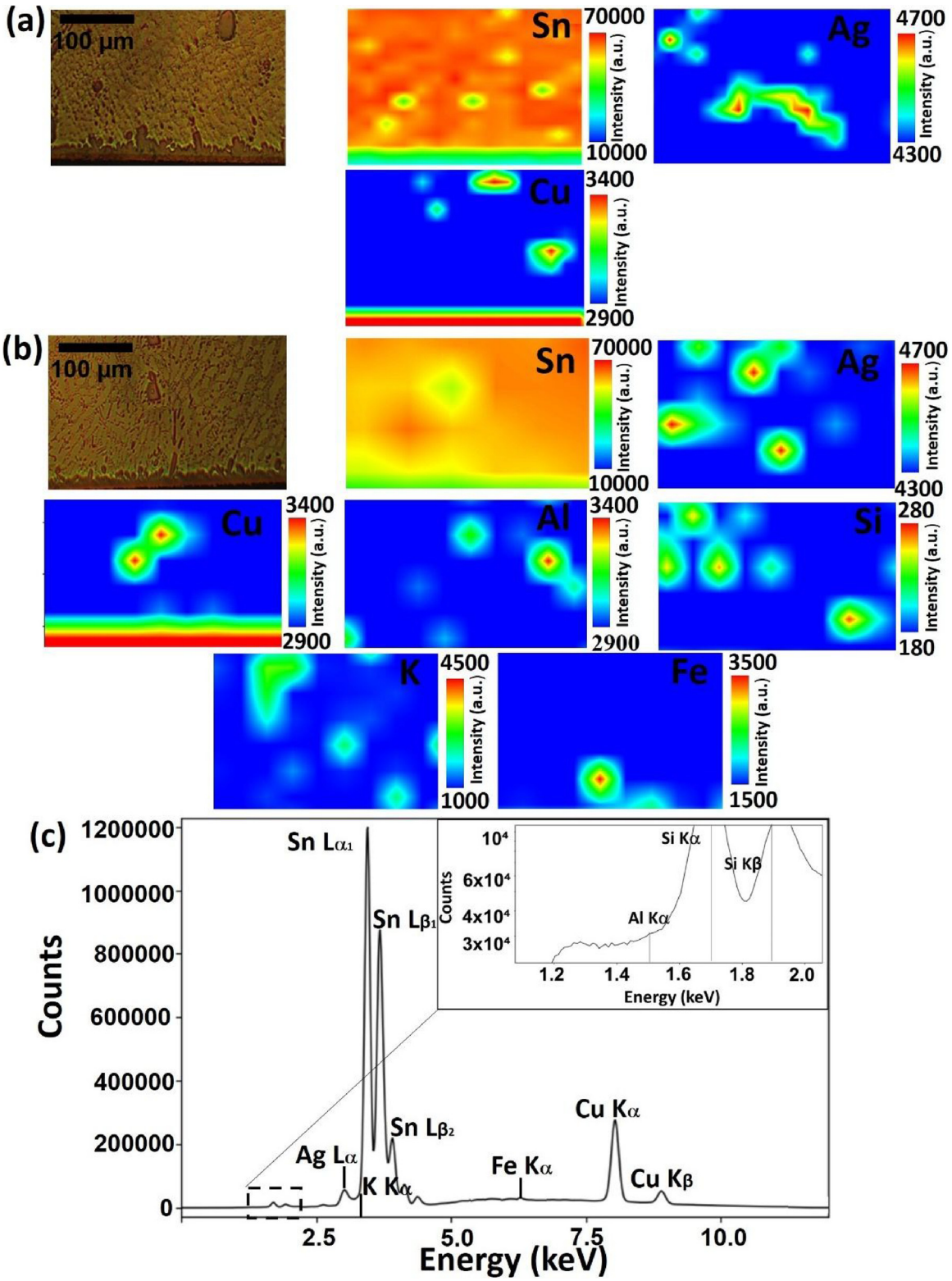

Fig. 8. The synchrotron micro-XRF mapping area of (a) pure SAC305, (b) KGC reinforced SAC305 composite solder and the (c) spectrum analysis of sample KGC reinforced SAC305 composite solder.

Further details of microstructure were analyzed using EBSD. The orientation of crystal structure in the pure SAC305 and in KGC reinforced SAC305 composite solder was investigated. The structure of beta-tin (β-Sn) is a body-centered tetragonal with lattice parameters of $a = 5.632$ nm, $c = 0.3182$ nm and $c/a = 0.546$ which possess anisotropic, thermal, mechanical and diffusion properties [37,38]. Since Sn grains are the main matrix in lead free solders, the orientation of the crystal structure may dictate the reliability of the solder joint. In this paper, β-Sn grain structures and grain orientations are the subject of interest since the structure of β-Sn may influence the mechanical response of solder joints under service conditions [39]. Fig. 9 shows EBSD maps and inverse pole figures of pure SAC305 and KGC reinforced

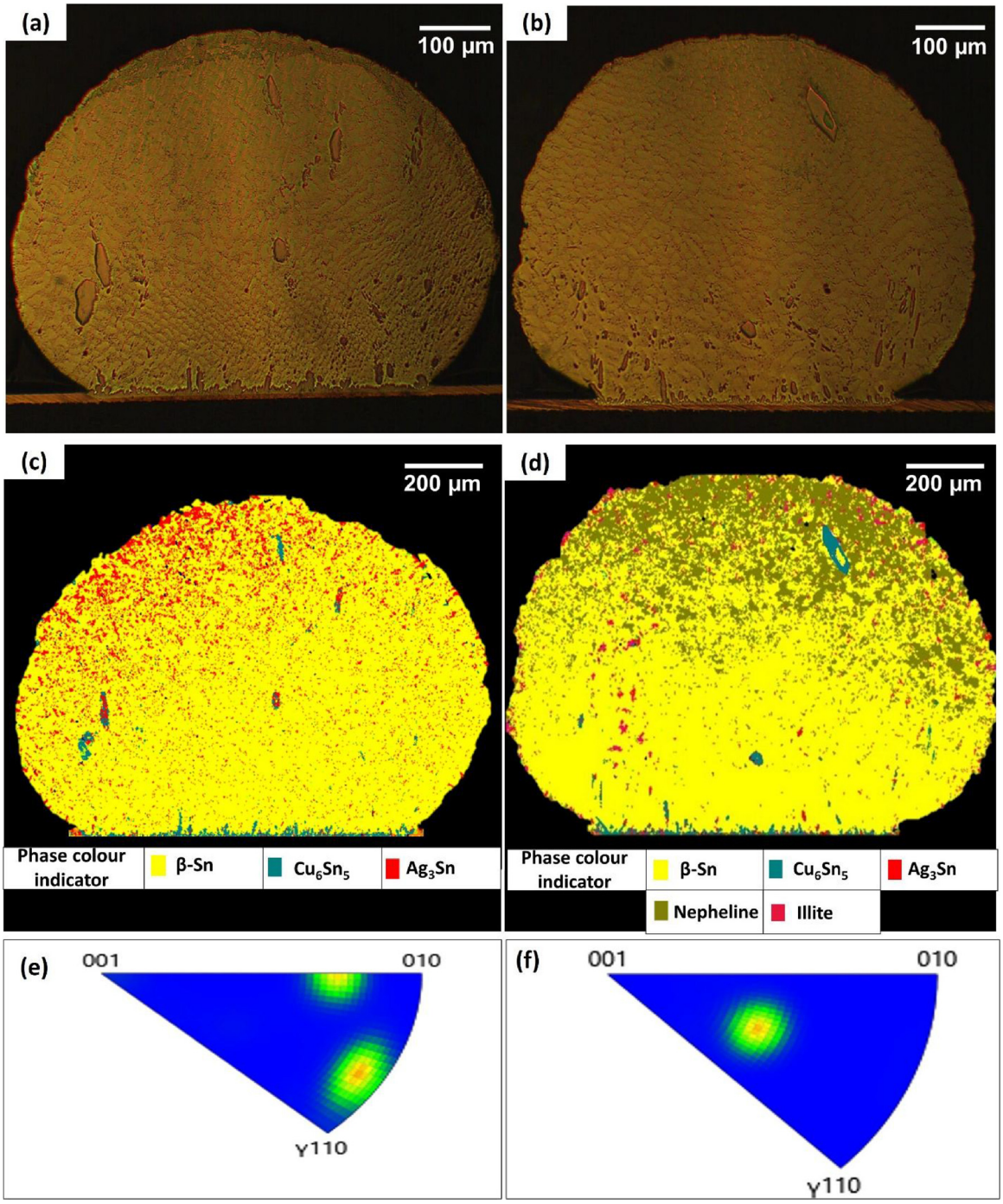

Fig. 9. Cross-sectioned optical microscope (OM) and electron backscatter diffraction (EBSD) image; (a) OM image of pure SAC305, (b) OM image of SAC305/1.0 wt.% KGC composite solder, (c) EBSD maps of pure SAC305, (d) EBSD maps of SAC305/1.0 wt.% KGC composite solder, (e) inverse pole figure (IPF-y) of pure SAC305, and (f) inverse pole figure (IPF-y) of SAC305/1.0 wt.% KGC composite solder.

SAC305 composite solder. The EBSD maps in Fig. 9(b) and (d) show that there are only single β-Sn crystals and no evidence of solidification twinning. By analyzing the inverse pole figure (IPF-y) in Fig. 9(e) and (f), the crystal orientations for the β-Sn crystal are [110] and [010]. However, small addition of KGC particles to SAC305 slightly changes the orientation of β-Sn crystal to single orientation of [001] as depicted in Fig. 9(f). Interestingly, Fig. 9(d) shows the existence of KGC crystalline phases, with the major phase as nepheline. According to Yun Ming et al. [30], crystalline nepheline is the major phase existing in KGC for heat-treated sodium based geopolymers.

Meanwhile, Fig. 10 shows the strain contouring maps of pure SAC305 and SAC305 with the addition of KGC particles. In order to quantitively measure the strain contouring area in both samples, the area fraction of strain contours were measured as presented in Fig. 10(c). By comparing the distribution of localized strain in both samples, pure SAC305 lead free solder has a lower distribution of localized strain than the sample with the addition of KGC particles. The area fraction of localized strain measured in the pure SAC305 and KGC reinforced SAC305 composite solder are 36,318 μm^2 and 72,188 μm^2, respectively. In addition, it can also be seen the distribution of localized strain in the SAC305 with KGC additions is more homogenous than in the pure SAC305 lead free solder. In the pure SAC305, the localized

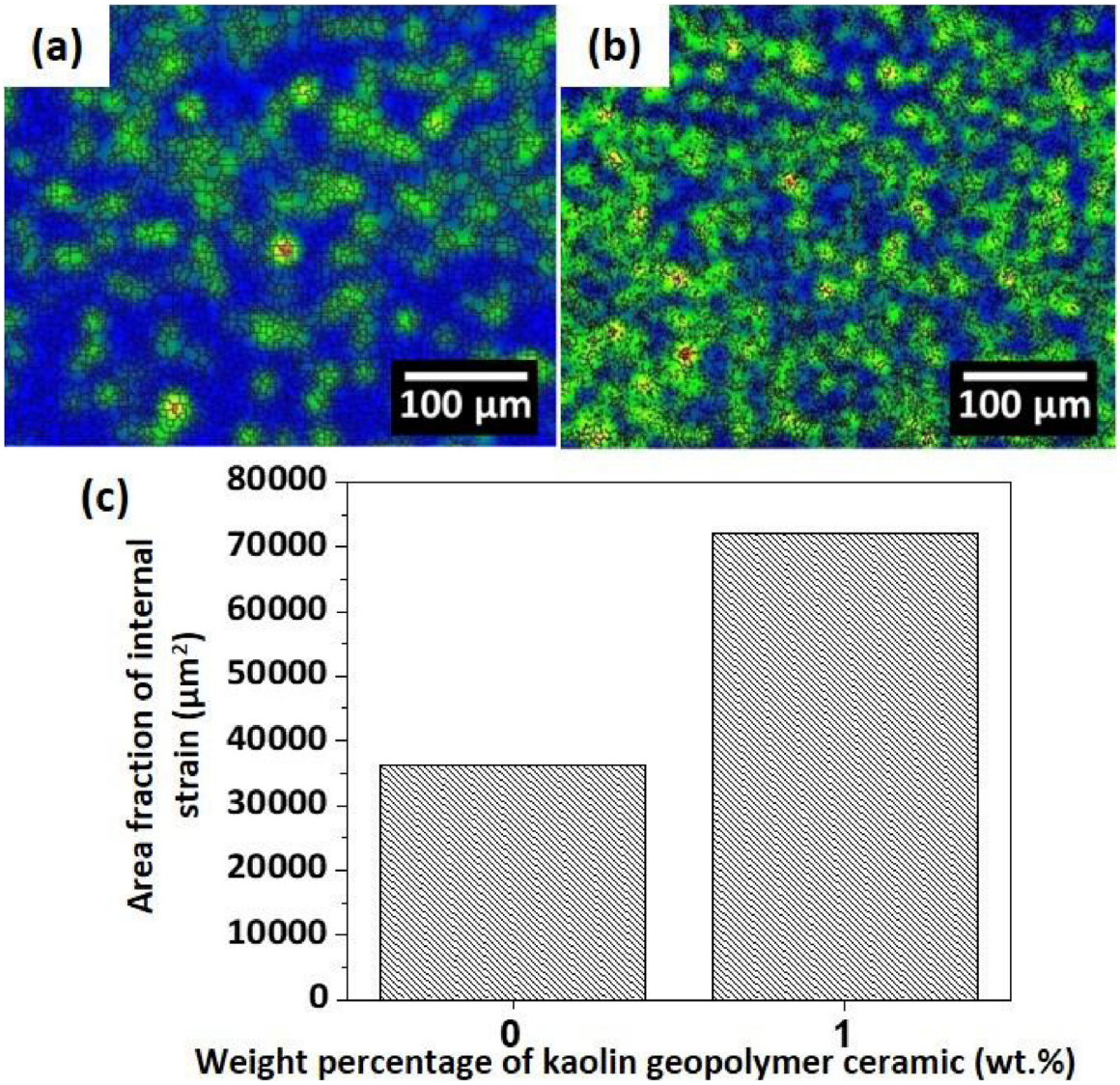

Fig. 10. Strain contour for (a) pure SAC305 and (b) SAC305/1.0 wt.% KGC composite solder and (c) area fraction of internal strain.

strain may be due to the inhomogeneity of Ag_3Sn and Cu_6Sn_5 intermetallics, while in the KGC reinforced SAC305 composite solder strain is mainly well distributed by the KGC reinforcement.

In order to investigate the interactions between the bulk KGC and SAC305 lead free solder, synchrotron micro-XRF analysis was conducted. Fig. 11 shows the results of synchrotron micro-XRF elemental mapping conducted on samples of SAC/KGC. The samples for synchrotron micro-XRF mapping consists of two parts: SAC305 lead free solder and KGC area as presented in Fig. 11(a). The red coloured regions indicate the highest concentration of the elements while blue coloured regions indicate the lowest concentration of the elements in that particular area. According to the elemental mapping in Fig. 11, it clearly shows that some elements, especially Al, Si and K from KGC systems migrated to the solder area. In addition, point analysis was carried out at "Point 1" to confirm the presence of particular elements in the solder area part. Based on the spectrum at Point 1, it was confirmed Al, Si and K elements from KGC systems existed in the solder area. However, in this study the main concern was the migration of Al and Si elements since these elements were major elements in the geopolymer systems which formed the backbone of geopolymer chain Si-O-Al and Si-O-Si bonds. The migration of some Al and Si elements to the solder area is believed to be due to the interactions of lead free solder elements and KGC elements as bulk KGC was dipped in molten solder at 250 °C. The heating process involved destabilized the KGC chains and thus promoted elemental migration towards the solder area. Nevertheless, Na elements in KGC could act as alkali modifiers which may break the Si-O-Si and Si-O-Al bonding and thus lead to the migration of some elements to the solder area [40]. However, the data obtained from this experiment was not enough to justify and definitively prove the migration mechanism, and further detailed investigations need to be carried out.

3.2. Spreadability

Solderability of solder can be evaluated through spreadability of solder on copper substrates subjected to reflow soldering. In general, solder alloys with higher spreading areas and lower contact angle are favored for reliable solder interconnections. In this paper, solderability of the pure SAC305 and composite SAC305 lead free solders were investigated by measuring the contact angle and spreading areas formed prior to the reflow soldering process. In our previous study [2], we reported on the solderability of the pure SAC305 and composite SAC305 with the addition of kaolin geopolymer ceramic (KGC) based on the contact angle. The contact angle between the molten solder alloy and Cu substrates is related with the spreading areas, thus an evaluation on the spreadability of solder took place. Fig. 12 presents the

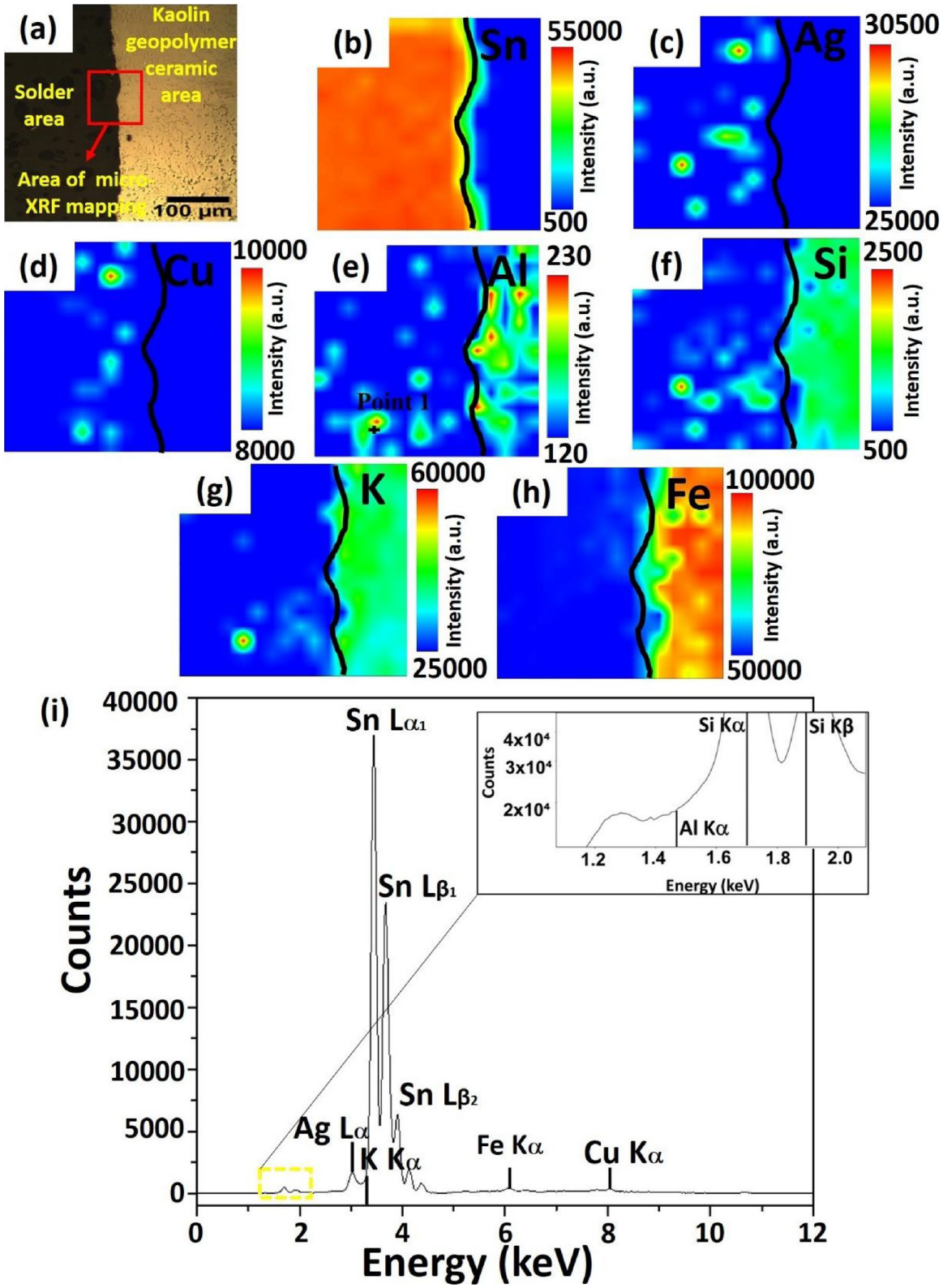

Fig. 11. Synchrotron micro-XRF results; (a) Image of synchrotron micro-XRF mapping area, (b) Sn, (c) Ag, (d) Cu, (e) Al, (f) Si, (g) K, (h) Fe elements mappings and (i) point analysis spectrum at Point 1.

spreadability of SAC305 with different addition of KGC on Cu substrates prior to reflow soldering process.

It was found that, the spreading areas increased and then decreased, with an increasing weight percentage (wt.%) of KGC particles. The spreading areas achieved maximum value of 91.45 mm^2 with the addition of 1.0 wt.% KGC, which is 23.6 % bigger than pure SAC305 lead free solder. However, the spreading area reduces for SAC305 with the addition of KGC up to 2.0 wt.%, to 80.40 mm^2 which is only 8.6 % bigger. Therefore, from the results it is inferred that smaller wt.% addition of KGC contributes to the improvement in ability of solder having

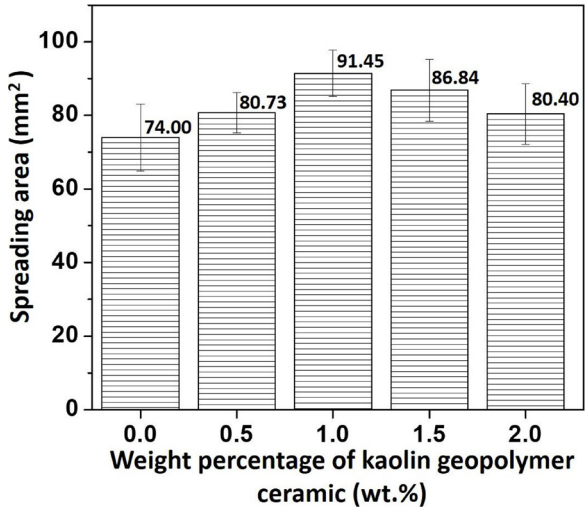

Fig. 12. Spreadability of SAC305 lead free solder with different weight percentages of KGC on a copper substrate.

bigger spreading on Cu substrates. One reason for this could be due to the added KGC particles lowering the interfacial surface energy and reducing surface tension as KGC particles accumulate at the interface between the flux and molten solder during the process of reflow soldering. In addition, as suggested by Chen at.al [21] and Sharma et.al [23], excess addition of reinforcements in solders can increase the viscosity of solder and obstruct the molten solder from further spreading. In conclusion, unappropriated amounts of reinforcements would deteriorate the solderability of solder alloys.

3.3. Thermal properties

Fig. 13 depicts the typical heating and cooling curve of the pure SAC305 solder and SAC305 composite solder with different wt.% of KGC addition. During the heating, a sharp endothermic peak was observed. Table 2 depicts the results obtained from DSC testing for the value of average undercooling, pasty range and melting temperature for the pure SAC305 and KGC reinforced SAC305 composite solders. These results show that, the addition of various amounts of KGC have little effect on the average melting point of SAC305 lead free solder alloys. Hence, the new composite solder system can be applied and integrated with the existing reflow profile during the soldering process without any major adjustments needed. The slight increase in the melting point of SAC305 lead free solder with the addition of KGC was possibly due to the reinforcing particles changing the surface instability and variation in the physical properties of grain boundary/interfacial characteristics. Besides that, KGC particles reinforced in SAC305 lead free solder retard the solidification process where it acts as retardation sites for the solidification process of IMCs [41]. These results are in good agreement with previous work reported [41,42].

Pasty range is an important thermal parameter in developing new composite solder alloys which can be measured by the difference between T_{endset} and T_{onset} during the heating process as presented in Table 2. In this study, the average pasty range of pure SAC305 lead free solder was 8.92 °C. While, KGC reinforced SAC305 composite solder with different wt. % of KGC showed no significant change in the average pasty range as compared to pure SAC305 solder. For these smaller pasty ranges it can be inferred that for the KGC reinforced SAC305 composite solder alloy, a partially liquid phase exists for a short time during the solidification process. This reduces the time of contact between the liquid phase and Cu substrates. Therefore, with a smaller pasty range, the interfacial IMC in the reinforced KGC SAC305 composite solder alloy is thinner in comparison to SAC305 lead free solder. Incidentally, a large pasty range can give rise to fabrication issues such as porosity, hot tearing contraction during solidification and fillet lifting phenomena [43], and these harmful issues will be reduced by the addition of geopolymer particles.

Thermodynamically, larger undercooling will result in a greater driving force for IMCs to grow. Undercooling is defined as the difference between T_{onset} during heating and T_{onset} during cooling, which is also related to the temperature range of solid phase nucleation in a liquid state until solidification [15]. The average undercooling of pure SAC305 and KGC reinforced SAC305 composite solders with different wt.% KGC is shown in Table 2. Based on the result, the undercooling of the pure SAC305 lead free solder is 19.64 °C. While for KGC reinforced SAC305 composite solder, the undercooling is in the range between 14.89–16.81 °C. The lowest undercooling of 14.89 °C was achieved with the addition of 1.0 wt.% KGC, a significant decrease of 24.2 %. This undercooling in the SAC305 with 1.0 wt.% KGC addition is very advantageous, since the undercooling in solder alloy will influence the microstructure formation. The reduction in the undercooling of KGC reinforced SAC305 composite solder affects the microstructure formation as discussed at Section 3.1 where the fraction of β-Sn phase decreased with smaller size of IMCs dispersed in eutectic area. The significant changes during undercooling can be attributed to the effect of the reinforcing particles. As suggested by El-Daly et.al. [15], the decrement in the undercooling of SAC105 with addition of SiC is due to the decreased in the undercooling of β-Sn which inhibits the formation of IMCs. By inducing higher nucleation, the solidification of β-Sn will be faster which reduces the time for any IMCs to grow, resulting in finer microstructures.

3.4. Mechanical properties

Mechanical properties of the SAC305/x-KGC composite solder and pure SAC305 solder joints were determined based on their shear strength and failure behaviors Fig. 14(a) illustrates the average shear strength results of SAC305/x-KGC composite solder. It can be seen that, the addition of various wt.% of KGC positively influenced the shear strength of solder joints. The average shear strength of KGC reinforced SAC305 composite solder increased with the addition of various wt.% KGC. Highest average shear strength was observed with the additions of 1 wt.% KGC with an average of 13.01 MPa compared to the non-added reinforcement solder with an average of 9.95 MPa. This is an increment of 31 % in the average shear strength as shown with additions of 1 wt.% KGC compared to SAC305 solder joints. However, with the addition of KGC beyond 1 wt.% (1.5 wt.% and 2.0 wt.%), the average shear strength of solder joints only slightly increased to 12.06 MPa and 10.32 MPa for 1.5 wt.% and 2.0 wt.% of KGC additions, respectively. The average shear strength of KGC reinforced SAC305 composite solders with lower KGC addition (0.5 wt.%) also increased to 12.34 MPa, indicating that all KGC additions increased the shear strength compared to SAC solder joints without any reinforcement.

In this paper, the enhancement in the shear strength of KGC reinforced SAC305 composite solders is attributable to the theory of dispersion strengthening. Based on the theory, the existence of fine Ag_3Sn and Cu_6Sn_5 intermetallic particles which were well dispersed into the β-Sn matrix strengthens the composite solders. In addition, KGC particles that were uniformly distributed along the grain boundaries of the solder hinder the dislocation movement and impede grain boundary sliding. The phenomenon in play is known as pinning effects, which can explain the improvement in the shear strength of composite solders. Also, the improvement in the shear strength of composite solders can also be attributed to the control of the thickness of IMC layer formation at the interface between the composite solders and the Cu substrate as suggested by Wu et al. [44]. A thicker IMC layer is prone to brittle failure that will degrade the strength of the solder joint. In this research, the thicknesses of IMC layers in KGC reinforced SAC305 composite solders were shown to decrease with the additions of KGC reinforcements, which partially improved the shear strength of the

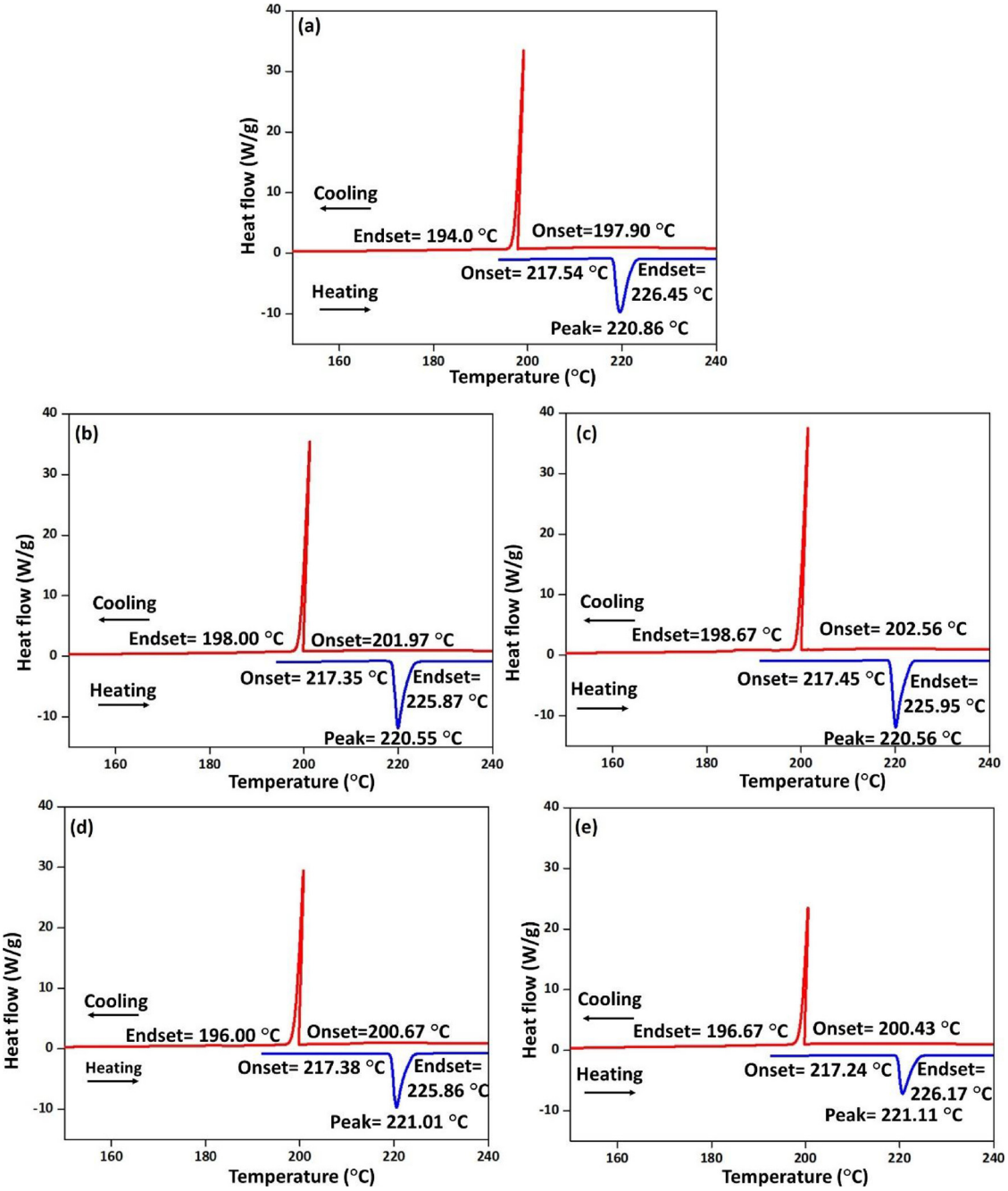

Fig. 13. Heating and cooling curve of SAC305 with different kaolin geopolymer ceramic weight percentage; (a) 0 wt.% KGC, (b) 0.5 wt.% KGC, (c) 1.0 wt.% KGC, (d) 1.5 wt.% KGC and (e) 2.0 wt.% KGC.

solder joints compared to pure SAC305 solder.

In order to further understand the failure behavior in KGC reinforced SAC305 composite solder and pure SAC305 solder, the post shear samples were examined. Fig. 14(b–f) shows the fracture surface for pure SAC305 and KGC reinforced SAC305 composite solders. Fig. 14(b) depicts the fracture behavior of pure SAC305 solder. It was observed that the pure SAC305 solder exhibits a combination of brittle and ductile fractured mode. Thus, the crack was believed to propagate from brittle IMC layer and moves to the solder bulk. Unalike, the fracture behavior of KGC reinforced SAC305 composite solders showed a transformation in the mode of fractured, from combination of brittle and ductile fracture mode to ductile mode. More dimples were observed in the samples containing KGC particles. The existence of more dimples correlates with better plastic properties for ductile materials. However, as the addition of KGC beyond 1.0 wt.%, large dimples were observed at the fracture surface which may explain the decrement in the shear strength of the samples at 1.5 wt.% and 2.0 wt.% of KGC additions.

4. Conclusions

The effects of adding kaolin geopolymer ceramic with various weight percentages to Sn-3.0Ag-0.5Cu solder was elucidated in this paper. It can be concluded that;

(a) The addition of KGC alters the microstructure formation by decreasing the formation of β-Sn area and increasing the eutectic area with fine intermetallics of Cu_6Sn_5 and Ag_3Sn. KGC addition reduces the thickness of interfacial IMC with formation of small rounded

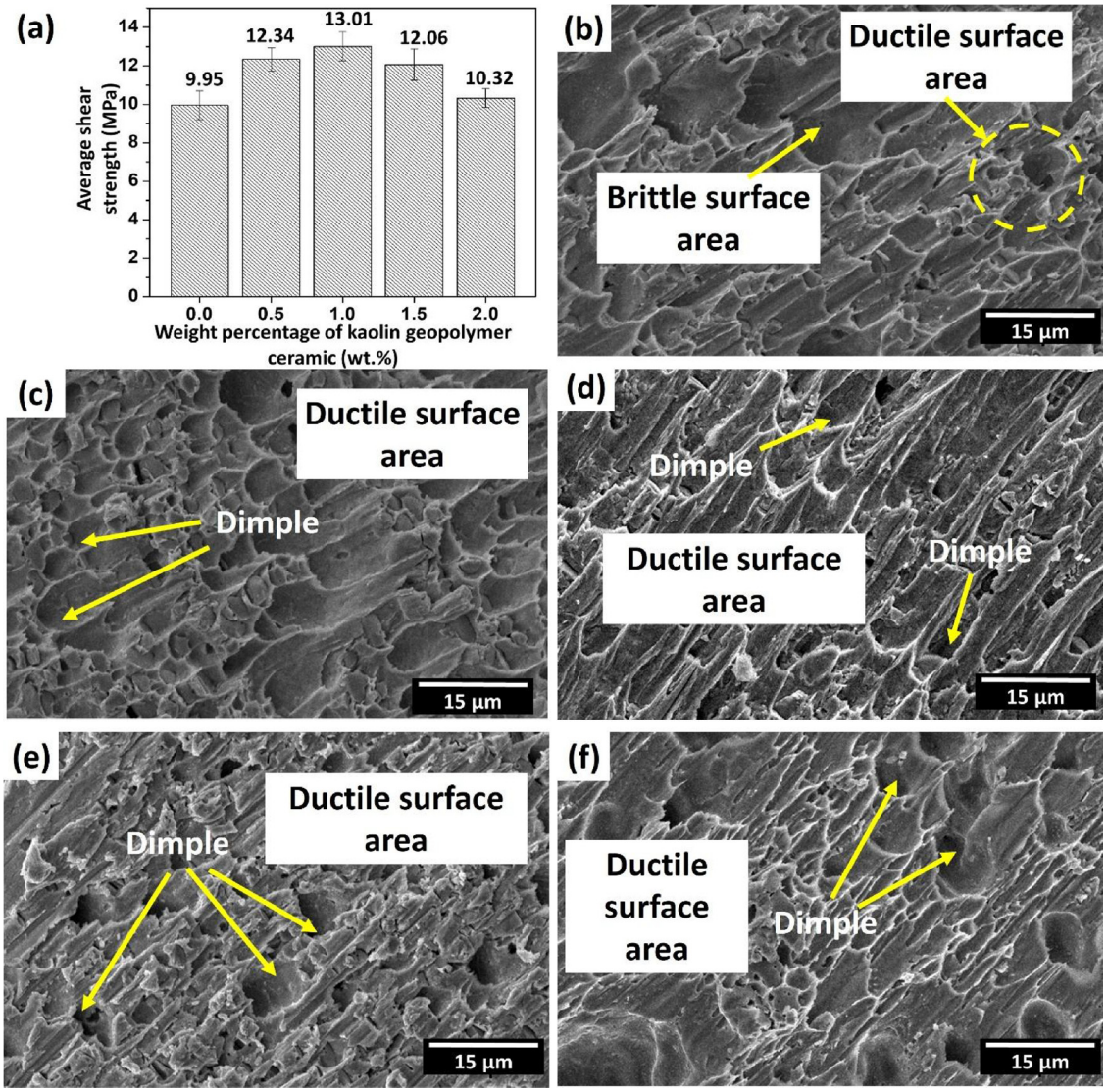

Fig. 14. (a) Average shear strength of SAC305 lead free solder with different wt.% KGC, SEM micrograph of fracture surfaces of pure SAC305 and KGC reinforced SAC305 composite solders at different weight percentage of KGC; (b) 0 wt. % KGC, (c) 0.5 wt.% KGC, (d) 1.0 wt.% KGC, (e) 1.5 wt.% KGC and (f) 2.0 wt.% KGC.

scallops. The optimum thickness was found to be an addition of 1.0 wt.% KGC. This was owing to the existence of KGC particles along the interfacial IMC acting as a barrier that reduces the Cu diffusion from the substrate to the SAC305 solder matrix that stabilizes and reduces the growth of interfacial IMC.

(b) Measurements by synchrotron micro-XRF confirmed that the distribution of KGC elements in the as-reflowed samples were mainly located at the solder bulk area. While EBSD testing showed that, the addition of KGC changes the orientation of β-Sn into single crystal orientation with a high area of localized strain contouring. The interaction of SAC305 solder alloy with bulk KGC leads to migration of elements Al and Si to the solder area part as Na elements in geopolymer system play a role as a bond breaker between Si-O-Si and Si-O-Al bonds.

(c) Improvement in the spreading area were achieved by the KGC addition, with the highest spreading area achieved with a 1.0 wt.% KGC addition. The average undercooling value was reduced by up to 24.2 % which is significant, with the lowest value of 14.89 °C achieved with 1.0 wt.% KGC addition. The reduction occurs due to the fact that KGC reinforcement plays a role in inducing higher nucleation and promoting faster solidification, which results in finer microstructures.

(d) The average shear strength of the SAC305 lead free solder with 1.0 wt.% KGC had the highest average strength of 13.01 MPa. This increment of 31 % in average shear strength compared to pure SAC305 lead free solder, proved the ability of KGC reinforcement in enhancing the mechanical properties of the composite SAC305 solder. In addition, small dimples with ductile failure mode were observed in the samples with 1.0 wt.% KGC addition.

Declaration of Competing Interest

The authors declare that they have no known competing financial interests or personal relationships that could have appeared to influence the work reported in this paper.

Acknowledgements

This work was supported by Ministry of Higher Education, Malaysia under the fundamental research grant scheme (FRGS) (FRGS/1/2017/TK10/UNIMAP/03/2)(9003-00612), Newton Fund Institutional Link Grant, ID 332397914, under the Newton-Ungku Omar Fund partnership. The grant is funded by the UK Department of Business, Energy and Industrial Strategy (BEIS) and Malaysiaand delivered by the British

Council.

Appendix A. Supplementary data

Supplementary material related to this article can be found, in the online version, at doi:https://doi.org/10.1016/j.mtcomm.2020.101469.

References

[1] N. Zaimi, et al., The effect of geopolymer ceramic additions to the wettability and shear strength of Sn-Ag-Cu (SAC) solder: a preliminary study, IOP Conference Series: Materials Science and Engineering 551 (2019) 012081.

[2] N.S.M. Zaimi, et al., Influence of kaolin geopolymer ceramic additions to the wettability and electrical properties of Sn-3.0Ag-0.5Cu (SAC305) lead free solder, IOP Conference Series: Materials Science and Engineering 701 (2019) 012033.

[3] X.D. Liu, et al., Effect of graphene nanosheets reinforcement on the performance of Sn-Ag-Cu lead-free solder, Mater. Sci. Eng. A 562 (Supplement C) (2013) 25–32.

[4] D.-H. Jung, A. Sharma, J.-P. Jung, Influence of dual ceramic nanomaterials on the solderability and interfacial reactions between lead-free Sn-Ag-Cu and a Cu conductor, J. Alloys. Compd. 743 (2018) 300–313.

[5] M.A.A. Mohd Salleh, et al., Development of a microwave sintered TiO2 reinforced Sn–0.7wt%Cu–0.05wt%Ni alloy, Mater. Des. 82 (2015) 136–147.

[6] R.J. Coyle, K. Sweatman, B. Arfaei, Thermal fatigue evaluation of Pb-Free solder joints: results, lessons learned, and future trends, JOM 67 (10) (2015) 2394–2415.

[7] Z.L. Ma, et al., Mechanisms of beta-Sn nucleation and microstructure evolution in Sn-Ag-Cu solders containing titanium, J. Alloys. Compd. (2018).

[8] Z.H. Li, et al., Effects of CeO2 nanoparticles addition on shear properties of low-silver Sn–0.3Ag–0.7Cu-xCeO2 solder alloys, J. Alloys. Compd. 789 (2019) 150–162.

[9] Z.H. Li, et al., A diffusion model and growth kinetics of interfacial intermetallic compounds in Sn-0.3Ag-0.7Cu and Sn-0.3Ag-0.7Cu-0.5CeO2 solder joints, J. Alloys. Compd. (2019) 152893.

[10] A.K. Gain, et al., Microstructure, kinetic analysis and hardness of Sn–Ag–Cu–1wt% nano-ZrO2 composite solder on OSP-Cu pads, J. Alloys. Compd. 509 (7) (2011) 3319–3325.

[11] A.K. Gain, Y.C. Chan, W.K.C. Yung, Effect of additions of ZrO2 nano-particles on the microstructure and shear strength of Sn–Ag–Cu solder on Au/Ni metallized Cu pads, Microelectron. Reliab. 51 (12) (2011) 2306–2313.

[12] S.S. Mohd Nasir, et al., Effect of TiO2 nanoparticles on the horizontal hardness properties of Sn-3.0Ag-0.5Cu-1.0TiO2 composite solder, Ceram. Int. 45 (15) (2019) 18563–18571.

[13] M.I.I. Ramli, et al., Effect of TiO2 additions on Sn-0.7Cu-0.05Ni lead-free composite solder, Microelectron. Reliab. 65 (2016) 255–264.

[14] M.A.A. Mohd Salleh, et al., Suppression of Cu6Sn5 in TiO2 reinforced solder joints after multiple reflow cycles, Mater. Des. 108 (2016) 418–428.

[15] A.A. El-Daly, et al., Novel SiC nanoparticles-containing Sn–1.0Ag–0.5Cu solder with good drop impact performance, Mater. Sci. Eng. A 578 (2013) 62–71.

[16] A.A. El-Daly, et al., Microstructural modifications and properties of SiC nanoparticles-reinforced Sn–3.0Ag–0.5Cu solder alloy, Materials & Design (1980-2015) 65 (2015) 1196–1204.

[17] M.A.A. Mohd Salleh, et al., Mechanical properties of Sn–0.7Cu/Si3N4 lead-free composite solder, Mater. Sci. Eng. A 556 (2012) 633–637.

[18] M.A.A, M.S, et al., Solderability of Sn-0.7Cu/Si3N4 lead-free composite solder on Cu-substrate, Phys. Procedia 22 (Supplement C) (2011) 299–304.

[19] F. Che Ani, et al., The influence of Fe2O3 nano-reinforced SAC lead-free solder in the ultra-fine electronics assembly, Int. J. Adv. Manuf. Technol. 96 (1) (2018) 717–733.

[20] T. Fouzder, et al., Influence of SrTiO3 nano-particles on the microstructure and shear strength of Sn–Ag–Cu solder on Au/Ni metallized Cu pads, J. Alloys. Compd. 509 (5) (2011) 1885–1892.

[21] G. Chen, et al., Performance of Sn–3.0Ag–0.5Cu composite solder with TiC reinforcement: physical properties, solderability and microstructural evolution under isothermal ageing, J. Alloys. Compd. 685 (2016) 680–689.

[22] Y. Wang, et al., Effects of nano-SiO2 particles addition on the microstructure, wettability, joint shear force and the interfacial IMC growth of Sn3.0Ag0.5Cu solder, J. Mater. Sci. Mater. Electron. 26 (12) (2015) 9387–9395.

[23] A. Sharma, B.G. Baek, J.P. Jung, Influence of La2O3 nanoparticle additions on microstructure, wetting, and tensile characteristics of Sn–Ag–Cu alloy, Mater. Des. 87 (Supplement C) (2015) 370–379.

[24] L.C. Tsao, et al., Effects of nano-Al2O3 particles on microstructure and mechanical properties of Sn3.5Ag0.5Cu composite solder ball grid array joints on Sn/Cu pads, Mater. Des. 50 (2013) 774–781.

[25] T.H. Chuang, et al., Strengthening mechanism of nano-Al2O3 particles reinforced Sn3.5Ag0.5Cu lead-free solder, J. Mater. Sci. Mater. Electron. 22 (8) (2011) 1021–1027.

[26] L.C. Tsao, et al., Effects of nano-Al2O3 additions on microstructure development and hardness of Sn3.5Ag0.5Cu solder, Mater. Des. 31 (10) (2010) 4831–4835.

[27] D. Dimas, I. Giannopoulou, D. Panias, Polymerization in sodium silicate solutions: a fundamental process in geopolymerization technology, J. Mater. Sci. 44 (2009) 3719–3730.

[28] N.A. Jaya, et al., Kaolin geopolymer as precursor to ceramic formation, MATEC Web Conf. 78 (2016) 01061.

[29] N.A. Jaya, et al., Characterization and microstructure of kaolin-based ceramic using geopolymerization, Key Eng. Mater. 700 (2016) 3–11.

[30] Y.M. Liew, et al., Formation of one-part-mixing geopolymers and geopolymer ceramics from geopolymer powder, Constr. Build. Mater. 156 (2017) 9–18.

[31] Na. Jaya, M.M.A.B. Abdullah, R. Ahmad, Reviews on clay geopolymer ceramic using powder metallurgy method, Mater. Sci. Forum 803 (2014) 81–87.

[32] Y. Tang, G.Y. Li, Y.C. Pan, Influence of TiO2 nanoparticles on IMC growth in Sn–3.0Ag–0.5Cu–xTiO2 solder joints in reflow process, J. Alloys. Compd. 554 (2013) 195–203.

[33] X. Wang, et al., Strengthening mechanism of SiC-particulate reinforced Sn–3.7Ag–0.9Zn lead-free solder, J. Alloys. Compd. 480 (2) (2009) 662–665.

[34] Z.L. Li, et al., Effect of nano-TiO2 addition on microstructural evolution of small solder joints, J. Mater. Sci. Mater. Electron. 27 (6) (2016) 6076–6087.

[35] M.A.A. Mohd Salleh, et al., Rapid Cu6Sn5 growth at liquid Sn/solid Cu interfaces, Scr. Mater. 100 (2015) 17–20.

[36] H.Y. Hsiao, et al., Inhibiting the consumption of Cu during multiple reflows of Pb-free solder on Cu, Scr. Mater. 65 (10) (2011) 907–910.

[37] Y.-A. Shen, C. Chen, Effect of Sn grain orientation on formation of Cu6Sn5 intermetallic compounds during electromigration, Scr. Mater. 128 (2017) 6–9.

[38] H. Chen, et al., Grain orientation evolution and deformation behaviors in Pb-Free solder interconnects under mechanical stresses, J. Electron. Mater. 40 (2011) 2445.

[39] L.P. Lehman, et al., Cyclic twin nucleation in tin-based solder alloys, Acta Mater. 58 (10) (2010) 3546–3556.

[40] H. Jabraoui, et al., Effect of sodium oxide modifier on structural and elastic properties of silicate glass, J. Phys. Chem. B 120 (2016).

[41] A. Fawzy, et al., Effect of ZnO nanoparticles addition on thermal, microstructure and tensile properties of Sn–3.5 Ag–0.5 Cu (SAC355) solder alloy, J. Mater. Sci. Mater. Electron. 24 (2013).

[42] L.C. Tsao, An investigation of microstructure and mechanical properties of novel Sn3.5Ag0.5Cu–XTiO2 composite solders as functions of alloy composition and cooling rate, Mater. Sci. Eng. A 529 (Supplement C) (2011) 41–48.

[43] E.A. Eid, A.M. Deghady, A.N. Fouda, Enhanced microstructural, thermal and tensile characteristics of heat treated Sn-5.0Sb-0.3Cu (SSC-503) Pb-free solder alloy under high pressure, Mater. Sci. Eng. A 743 (2019) 726–732.

[44] N. Wu, S. Ismathullakhan, Y. Chan, Effect of 1 wt% ZnO nanoparticles addition on the microstructure, IMC development, and mechanical properties of high Bi content Sn–57.6Bi–0.4Ag solder on Ni metalized Cu pads, J. Mater. Sci. Mater. Electron. 25 (2014) 2169–2176.